NBS BUILDING SCIENCE SERIES 137

An Evaluation of Thermal Energy Conservation Schemes n Experimental Masonry Building

ARTMENT OF COMMERCE • NATIONAL BUREAU OF STANDARDS

NATIONAL BUREAU OF STANDARDS

The National Bureau of Standards[1] was established by an act of Congress on March 3, 1901. The Bureau's overall goal is to strengthen and advance the Nation's science and technology and facilitate their effective application for public benefit. To this end, the Bureau conducts research and provides: (1) a basis for the Nation's physical measurement system, (2) scientific and technological services for industry and government, (3) a technical basis for equity in trade, and (4) technical services to promote public safety. The Bureau's technical work is performed by the National Measurement Laboratory, the National Engineering Laboratory, and the Institute for Computer Sciences and Technology.

THE NATIONAL MEASUREMENT LABORATORY provides the national system of physical and chemical and materials measurement; coordinates the system with measurement systems of other nations and furnishes essential services leading to accurate and uniform physical and chemical measurement throughout the Nation's scientific community, industry, and commerce; conducts materials research leading to improved methods of measurement, standards, and data on the properties of materials needed by industry, commerce, educational institutions, and Government; provides advisory and research services to other Government agencies; develops, produces, and distributes Standard Reference Materials; and provides calibration services. The Laboratory consists of the following centers:

Absolute Physical Quantities[2] — Radiation Research — Chemical Physics — Analytical Chemistry — Materials Science

THE NATIONAL ENGINEERING LABORATORY provides technology and technical services to the public and private sectors to address national needs and to solve national problems; conducts research in engineering and applied science in support of these efforts; builds and maintains competence in the necessary disciplines required to carry out this research and technical service; develops engineering data and measurement capabilities; provides engineering measurement traceability services; develops test methods and proposes engineering standards and code changes; develops and proposes new engineering practices; and develops and improves mechanisms to transfer results of its research to the ultimate user. The Laboratory consists of the following centers:

Applied Mathematics — Electronics and Electrical Engineering[2] — Manufacturing Engineering — Building Technology — Fire Research — Chemical Engineering[2]

THE INSTITUTE FOR COMPUTER SCIENCES AND TECHNOLOGY conducts research and provides scientific and technical services to aid Federal agencies in the selection, acquisition, application, and use of computer technology to improve effectiveness and economy in Government operations in accordance with Public Law 89-306 (40 U.S.C. 759), relevant Executive Orders, and other directives; carries out this mission by managing the Federal Information Processing Standards Program, developing Federal ADP standards guidelines, and managing Federal participation in ADP voluntary standardization activities; provides scientific and technological advisory services and assistance to Federal agencies; and provides the technical foundation for computer-related policies of the Federal Government. The Institute consists of the following centers:

Programming Science and Technology — Computer Systems Engineering.

[1]Headquarters and Laboratories at Gaithersburg, MD, unless otherwise noted; mailing address Washington, DC 20234.
[2]Some divisions within the center are located at Boulder, CO 80303.

NBS BUILDING SCIENCE SERIES 137

An Evaluation of Thermal Energy Conservation Schemes for an Experimental Masonry Building

Parambir S. Gujral and Raymond J. Clark

Skidmore, Owings & Merrill
33 W. Monroe Street
Chicago, IL 60603

Douglas M. Burch

Center for Building Technology
National Engineering Laboratory
National Bureau of Standards
Washington, DC 20234

Sponsored by:
Skidmore, Owings & Merrill
National Bureau of Standards
and
King Abdul Aziz University
Makkah Campus
Saudi Arabia

U.S. DEPARTMENT OF COMMERCE, Malcolm Baldrige, Secretary
NATIONAL BUREAU OF STANDARDS, Ernest Ambler, Director

Issued July 1982

Library of Congress Catalog Card Number: 81-600175

National Bureau of Standards Building Science Series 137
Nat. Bur. Stand. (U.S.), Bldg. Sci. Ser. 137, 39 pages (July 1982)
CODEN: BSSNBV

U.S. GOVERNMENT PRINTING OFFICE
WASHINGTON: 1982

For sale by the Superintendent of Documents, U.S. Government Printing Office, Washington, DC 20402
Price $4.75
(Add 25 percent for other than U.S. mailing)

ABSTRACT

A one-room masonry building with exterior polystyrene rigid board insulation was built within a large environmental chamber at the National Bureau of Standards. Various climatic conditions were simulated within the chamber, and the transient thermal response of the test building was monitored. Three schemes (night cooling using a ceiling-mounted valance cooling coil, natural ventilation night cooling, and passive solar heating) were investigated with regard to energy conservation. The test results indicated that these operating practices resulted in a considerable reduction in energy consumption for space heating and cooling.

The measured performance of the test building compared favorably with the corresponding performance obtained with an analytic model.

Key words: building thermal mass; dynamic performance of buildings; energy conservation; heat transfer in buildings; night ventilation; night space cooling; passive solar heating.

ACKNOWLEDGMENTS

The authors would like to thank Dr. Jafar Sabbagh, Vice Chancellor of King Abdul Aziz University, for his contribution to the project development, and Mr. Robert Jones of the National Bureau of Standards for Project Administration. Also, appreciation is expressed to Mark LeMay for his technical assistance in the installation of the instrumentation, to Dave Ward and Doug Grant for operating the environmental chamber which simulated the weather cycles, and to Mrs. Mary Reppert for editing this manuscript.

In addition, the authors would like to express special thanks to the *National Concrete Masonry Association, Brick Institute of America, Pella Rolscreen Company, Dow Chemical U.S.A., Edwards Engineering Corporation, Hale Engineering Company, Inc., Flexicore Company, Inc.,* for donating building materials used for construction of the test building, and to *Kettler Brothers, Inc.,* for building the test building.

CONTENTS

Figures

Tables

1. INTRODUCTION

This study investigates the temperature response of a prototype dormitory building for a Saudi Arabian university. The university buildings were designed to incorporate a number of energy-saving concepts, some of which are reported herein. The campus is to be built in Makkah, Saudi Arabia, where the climate is essentially a summer condition for the entire year and an extreme summer condition for most of the year. The test building was built at the National Bureau of Standards within a high-bay environmental chamber in which various diurnal temperature cycles for Makkah were simulated. The test building was a one-room structure with massive masonry walls insulated from the environment by polystyrene board insulation placed exterior to the masonry. This type of construction creates a large amount of thermal storage capacity at the interior of the building which may be used to save substantial energy throughout the year. Three energy-savings schemes were investigated and are described below.

The first scheme investigated was night cooling using a ceiling-mounted valance cooling coil. This coil exchanged heat with the indoor air by means of convection. For this scheme, the test building was cooled during a nighttime period during which the interior surfaces of the walls, floor, and ceiling were cooled. During the day when the cooling system was not operated, the interior mass absorbed heat and thereby maintained a comfortable indoor condition. This study investigated the 24-hour indoor temperature response of the test building when it was cooled for 9- and 12-hour periods at night.

This scheme can be used in situations where a large group of buildings is served by a single central cooling plant. In such a situation, different sets of buildings serviced by a plant may be cooled at different times during a 24-hour period, thereby distributing the cooling load more uniformly and substantially reducing the peak load of the central plant. The

concept is particularly applicable to academic campuses where the occupancy normally shifts between classrooms and dormitories at times coincident with the space cooling schedule. In this way, the buildings are unoccupied during system off periods and occupied during system on periods.

The second scheme investigated was the use of night ventilation to cool the interior mass during the night hours. Night ventilation was accomplished by opening the windows and door and operating a ceiling fan to increase the rate of natural ventilation. During daytime periods, the interior mass absorbs heat and maintains comfortable conditions. During winter months in Makkah, the high daytime temperatures produce large cooling loads. However, the nighttime air frequently falls below a room comfort condition of 80 °F (27 °C). It has been theoretically shown [1]* that this cool night air may be used to cool the interior mass of a building and thereby provide "free" cooling. This study investigated the 24-hour indoor temperature response of the test building cooled in this fashion. It was shown that such a procedure has the potential of essentially eliminating air conditioning energy consumption during certain times of the year that ordinarily require substantial mechanical cooling.

A third energy-conservation scheme investigated was passive solar heating of the test building. This procedure is most applicable to the case of a passive solar house. A test was carried out in which the test building was exposed to a simulated window solar gain (using infrared heat lamps) for a mid-western U.S. climate, and the diurnal indoor temperature response was monitored.

* Numbers in brackets are references cited at the end of the report.

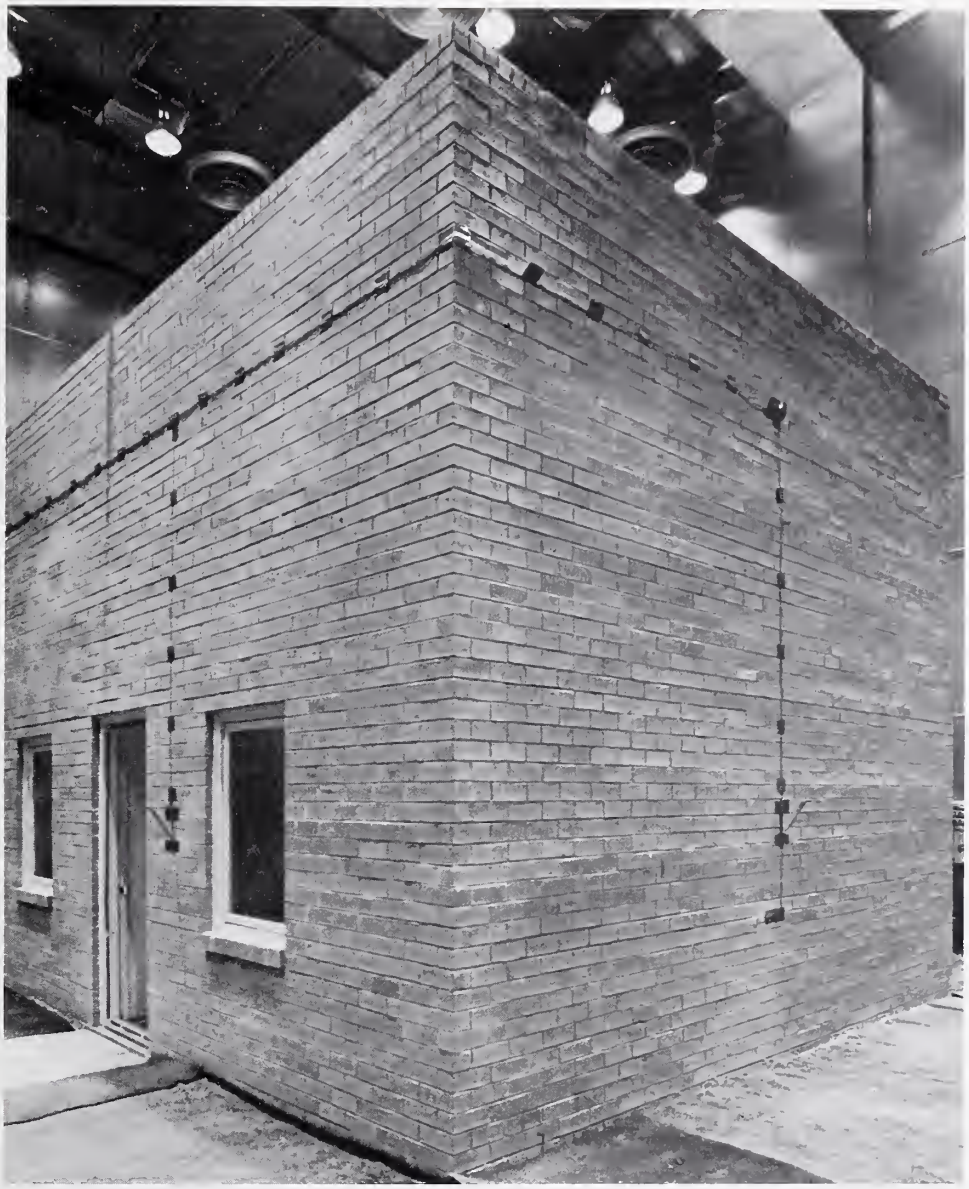

2. DESCRIPTION OF TEST BUILDING

A one-room test building was built within an environmental chamber at the National Bureau of Standards. The external dimensions of the test building were 21-ft 4-in (6.50 m) long by 17-ft 4-in (5.28 m) wide by 15-ft 2-in (4.62 m) high to the top of the parapet. The inside ceiling height was 13-ft 4-in (4.06 m). The building contained a door and two windows on one wall and three windows in the opposite wall. A photograph of the completed building is given above. A photograph of the building under construction is given in figure 1. The wall construction, from outside to inside, consisted of nominal 4-in (10 cm) face brick, an air space, 3 1/2-in (8.9 cm) rigid polystyrene insulation fastened to nominal 8-in (20 cm) solid concrete block with metal ties and 3/4-in (2 cm) plaster applied to the interior surface of the concrete block (see fig. 1). The total wall thickness was 16 7/8 in (43 cm).

FIGURE 1. PHOTOGRAPH OF THE TEST BUILDING DURING CONSTRUCTION

The roof consisted of concrete block pavers placed over 4-in (10 cm) polystyrene board insulation, which in turn was placed on 8-in (20 cm) precast hollow-core concrete panels spanning the short dimension of the building. A layer of 3/4-in (2 cm) plaster was applied to the inside ceiling surface, giving a total roof thickness of 14 3/8 in (37 cm).*

A 5 in (13 cm) thick concrete floor slab was poured over 4-in (10 cm) polystyrene board insulation placed over a compacted gravel bed. Thin-set quarry tile was mounted atop the concrete slab. The floor was insulated from the ground in order to simulate the thermal performance of the top floor of a three-story building.

The five windows were single-pane casement type. A removable second pane of glass was located at the interior side of the window. The windows contained complete weatherstripping with latches. The solid wooden door was weatherstripped.

A valance chilled-water cooling coil was installed below the ceiling. This unit was 18 ft (5.5 m) long and contained an eight-row coil. A drain pan under the coil was used to collect moisture condensed from the room air. A photograph of the valance coil with drain pan removed is shown in figure 2.

When in operation, the valance cooling coil creates cool natural convection air currents within the space. These currents are induced by buoyant forces caused by temperature differences within the interior space of the test building. Such a system does not require a fan or blower. A ceiling fan was installed within the structure to increase air movement during periods when the valance coil was not operated.

FIGURE 2. PHOTOGRAPH OF THE INTERIOR OF THE TEST BUILDING SHOWING THE VALANCE COOLING COIL

* A roof membrane was not included on the test building. However, one is normally included on such a building constructed in the field.

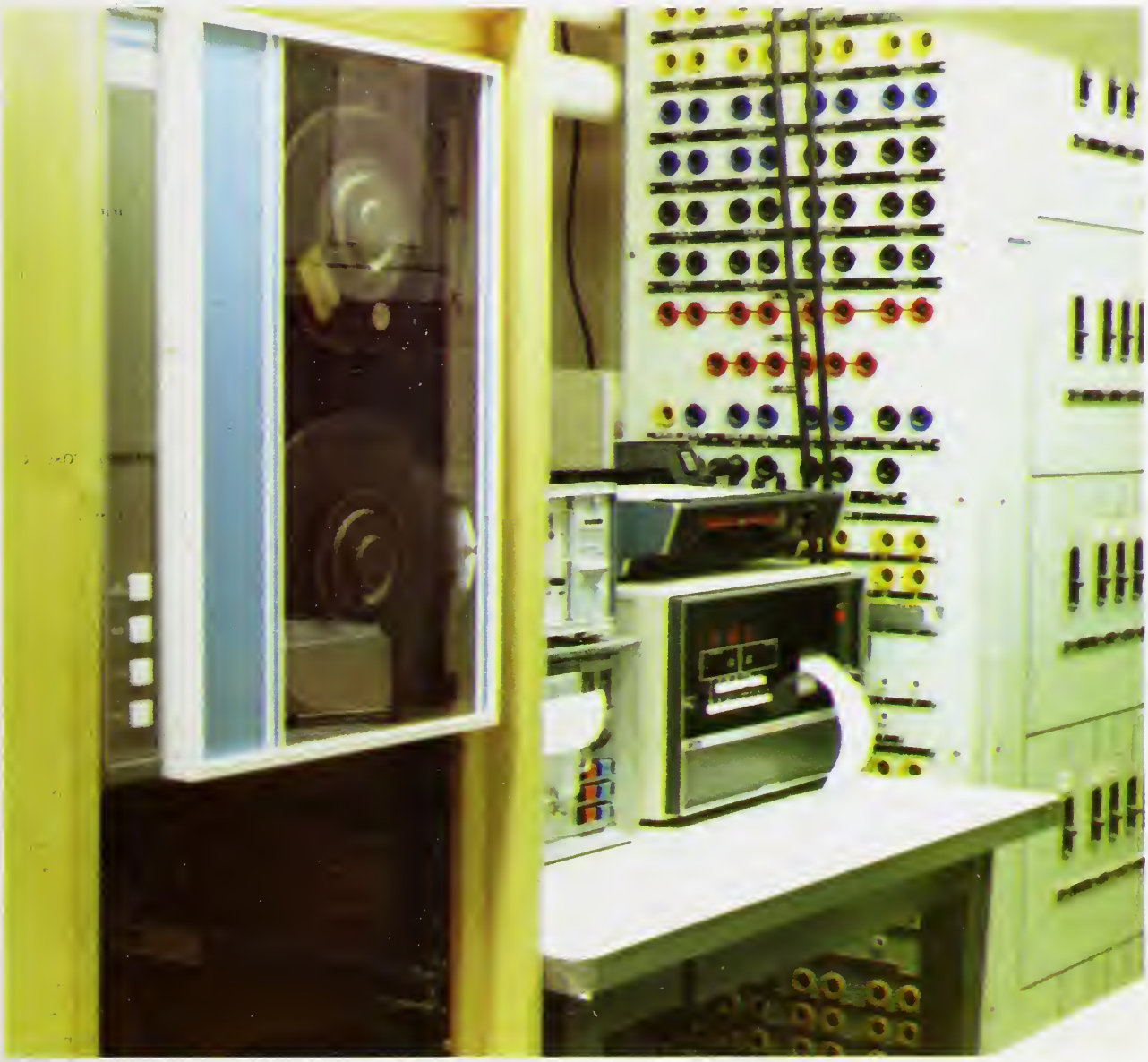

3. INSTRUMENTATION AND MEASUREMENT TECHNIQUE

Twenty-four-gage copper-constantan thermocouples were mounted at various locations throughout the test building to monitor the indoor temperature. Thermocouples were placed at the inside and outside surfaces of the roof and the four walls. These thermocouples were centrally located and attached to the building surfaces with epoxy. For each surface thermocouple, there is a second thermocouple located approximately 1 ft (30 cm) from the surface to sense the air temperature. The east wall contains two additional thermocouples, one located between the insulation and the concrete block, the other attached to the inside surface of the face brick. Thermocouples were also centrally located on the top and bottom sides of the rigid floor insulation to sense the one-dimensional heat transmission through the center portion of the floor slab. The thermocouple locations are depicted in figure 3.

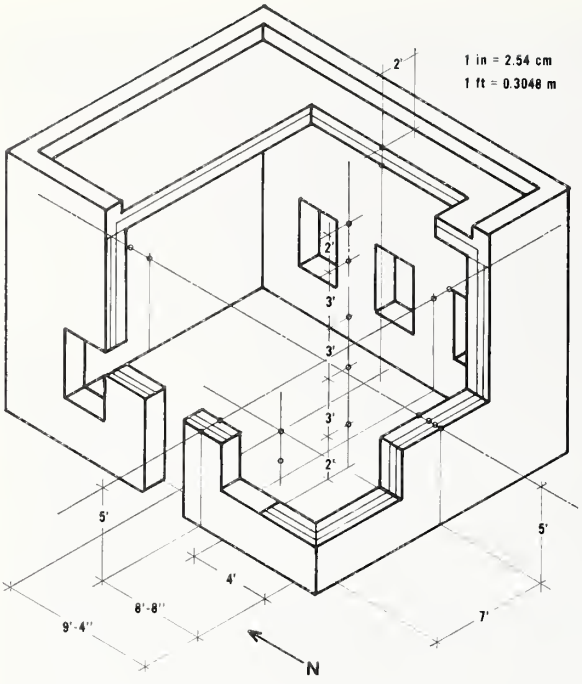

FIGURE 3. ISOMETRIC VIEW OF THE TEST BUILDING SHOWING THE THERMOCOUPLE LOCATIONS

A vertical column extending from the floor to the ceiling was located at a point 4 ft (1.2 m) in from the center of the south-facing wall. Thermocouples were located along this column at heights of 2, 5, 8, and 11 ft (0.6, 1.5, 2.4, and 3.4 m) above the floor to measure the floor-to-ceiling temperature gradient. A Dunmore-type relative humidity transducer was also located on the vertical column at a height of 4 ft (1.2 m) above the floor. This transducer, with potentiometer and power source, produced a millivolt signal proportional to the indoor relative humidity.

These transducers were connected to a 100-channel data acquisition system (DAS) located in the control room of the environmental chamber. The DAS contained an internal electronic ice-point reference. The channels of the DAS could be programed to output in millivolts, degrees Celsius, or degrees Fahrenheit. Recordings were printed at 30-minute intervals.

The rate of total heat removed (q) from the valance cooling coil was determined from the relation:

$$q = m \cdot c_p \cdot (T_o - T_i) \qquad (1)$$

where

m = mass flow rate of chilled water;
c_p = specific heat of water; and
$T_o - T_i$ = temperature rise of chilled water across coil.

The temperature rise ($T_o - T_i$) through the chilled water cooling coil was measured with a thermopile. This thermopile consisted of 10 thermocouple junctions. Five of these junctions were installed in a thermocouple well protruding into the supply line approximately 1 ft (30 cm) from the test building. The other five junctions were installed in a similar thermocouple well protruding into the return line. The output of this thermopile was measured with a strip chart recorder and a digital voltmeter.

A water flowmeter was installed in the supply line of the cooling coil. This meter produced a contact closure for each metered gallon of water. The output of the meter was connected to a pulse counting system which printed the number of hourly accumulated contact closures.

A condensate collection system was installed to determine the weight of condensate collected. This system did not function as it was intended, because water drained from the fins of the cooling coil only after it became saturated with water.

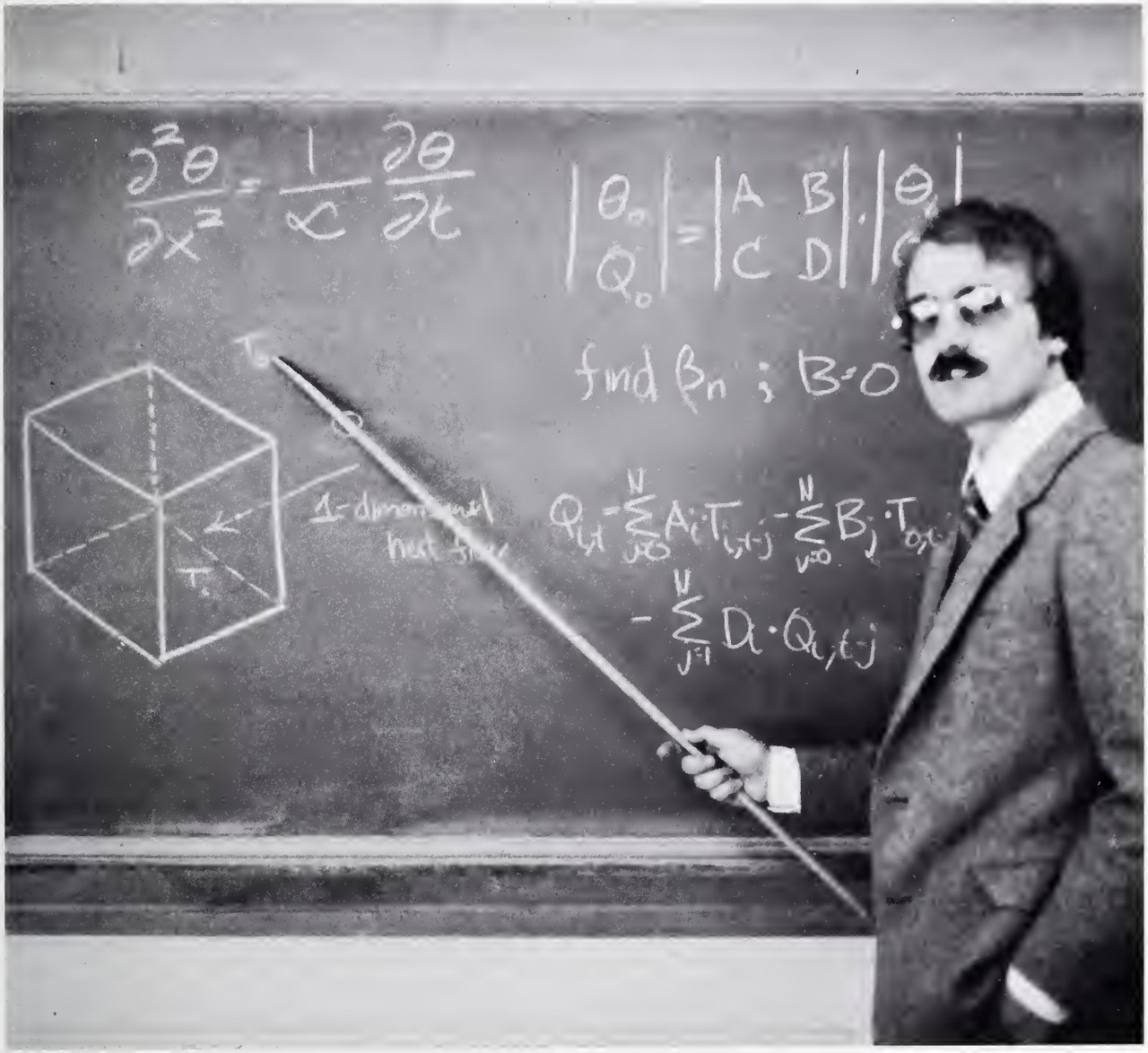

4. MATHEMATICAL MODEL

The theoretical performance of the test building was predicted using a mathematical model which performed a simultaneous heat balance at 15 building surfaces and the indoor air of the test building. The surfaces included the inside and outside wall for the four wall orientations, the inside and outside roof, the inside floor, and the windows and door for the four wall orientations. The resulting 16 simultaneous linear equations were solved by matrix inversion on a digital computer.

The following heat-transfer assumptions were made in the mathematical analysis:

1. the heat flow through all building surfaces is one-dimensional;
2. heat transfer properties of building materials are constant;
3. the indoor air is perfectly mixed (i.e., indoor air temperature is uniform);
4. infiltration rate is constant;
5. indoor air has negligible thermal storage capacity; and
6. the thermal storage capacities of the windows and door are negligible.

A single heat balance was used at each indoor and outdoor surface assuming a uniform temperature across the entire surface. A thermographic survey (see appendix A) of the inside surfaces of the test building showed this assumption to be valid except for the narrow region where the walls joined the ceiling. The time series heat conduction equation for the indoor and outdoor opaque building surfaces was taken from ref. [2] and is given below:

Indoor Surface

$$Q_{i,t} = \sum_{j=0}^{N} A_j \cdot T_{i,t-j} - \sum_{j=0}^{N} B_j \cdot T_{o,t-j} - \sum_{j=1}^{N} D_j \cdot Q_{i,t-j} \qquad (2)$$

where

$Q_{i,t}$ = heat transferred through the indoor surface at time t;
$T_{i,t-j}$ = temperature of indoor surface at time $t-j$;
$T_{o,t-j}$ = temperature of outdoor surface at time $t-j$; and
$Q_{i,t-j}$ = heat transferred through the indoor surface at time $t-j$.

Outdoor Surface

$$Q_{o,t} = \sum_{j=0}^{N} B_j \cdot T_{i,t-j} - \sum_{j=0}^{N} C_j \cdot T_{o,t-j} - \sum_{j=1}^{N} D_j \cdot Q_{o,t-j} \qquad (3)$$

where

$Q_{o,t}$ = heat transferred through the outdoor surface at time t; and
$Q_{o,t-j}$ = heat transferred through the outdoor surface at time $t-j$.

In eq. (2) and (3), A_j, B_j, C_j, and D_j, (for $j=0,1,2, \ldots N$) are the modified conduction transfer functions according to Mitalas and Arsenault [3].

The five windows and door were assumed to have negligible thermal storage. The heat balance equation used for these surfaces is given below:

$$Q_{q,t} = (T_{r,t}-T_{q,t})/R_r = (T_{q,t}-T_{c,t})/R_c \qquad (4)$$

where

$Q_{q,t}$ = heat transferred through the thermally quick* surfaces at time t;
$T_{c,t}$ = temperature of the environment chamber air
$T_{q,t}$ = temperature of the quick surface at time t; and
$T_{r,t}$ = temperature of the room air at time t.

The chamber and room thermal resistance values (R_c and R_r) given in eq (4) are the summation of the conduction and the convection-radiation components.

$$R_r = 1/h_i + R_s \qquad (5)$$

$$R_c = 1/h_o \qquad (6)$$

where

h_i = combined convection-radiation coefficient at the indoor surface; and
h_o = combined convection-radiation coefficient at the outdoor surface.

R_s = surface-to-surface thermal resistance of quick surface.

The heat balance for the indoor air of the test building contains terms describing the heat transferred from the massive and quick indoor surfaces, the heat contribution of infiltrating air, and the heat added by the simulated occupancy load, or:

$$O = \sum_{j=1}^{P} h_{j,t} \cdot S_j \cdot (T_{j,t}-T_{r,t}) + m_a \cdot c_p \cdot (T_{c,t}-T_{r,t}) + Q_p + Q_s \qquad (7)$$

where

P = the number of internal surfaces;
$h_{j,t}$ = combined convection-radiation coefficient for the jth surface;

* Here the term "quick" refers to surfaces with negligible thermal heat capacity.

S_j = area of jth surface perpendicular to heat flow;
$T_{j,t}$ = temperature of jth surface at time t;
m_a = mass flow rate of infiltrating air;
c_p = specific heat of air;
Q_p = occupant sensible heat gain; and
Q_s = sensible heat gain or loss from air conditioning system.

The sensible total cooling load (Q_s) served as an input for the mathematical model.

For each of the tests, the test building was exposed to a diurnal sol-air temperature cycle. This sol-air temperature cycle was determined by area-averaging the sol-air temperature for each of the building surfaces, or:

$$T_t = \frac{1}{S_T} \sum_{j=1}^{5} (T_{j,t} \cdot S_j) \tag{8}$$

where

T_t = area-averaged sol-air temperature at time t, and
S_j = area of jth surface.
S_T = total area

The sol-air temperature ($T_{j,t}$) for each of the surfaces (i.e., four walls and the roof) was determined from the procedures given in ref. [5].

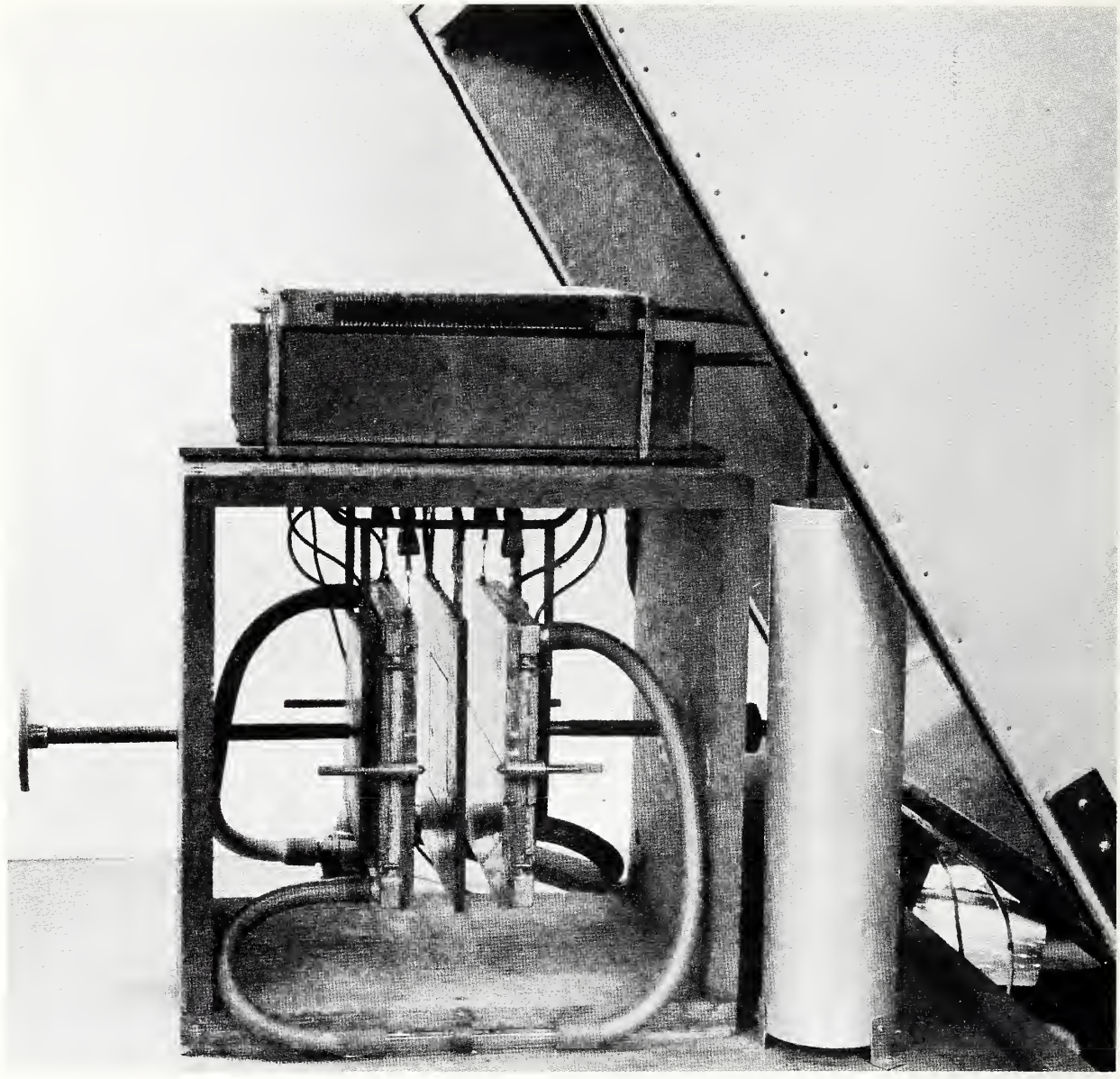

5. HEAT-TRANSFER PARAMETERS

The heat-transfer properties of the building materials used in the analysis are summarized in table 1. The areas used to compute heat flows through the building components were the exterior areas for each of the building components. These areas are summarized in table 2.

The coefficient of transmission for the solid wooden door was taken to be 0.47 Btu/hr·ft^2·°F (2.6 W/m^2·K). This value is based on data contained in ref. [5]. The coefficient of transmission for the windows was taken to be 0.44 Btu/hr·ft^2·°F (2.5 W/m^2·K). This value is based on data supplied by the window manufacturer.

Table 1. HEAT-TRANSFER PROPERTIES* OF BUILDING MATERIALS

Material	Thickness		Conductivity		Density		Specific Heat	
	in	(cm)	Btu/hr·ft·°F	(W/m·K)	lb/ft^3	(kg/m^3)	Btu/lb·°F	(J/Kg·K)
Face brick	3.5	(8.9)	.75	(1.30)	130.	(2080)	.20	(840)
Polystyrene insulation	3.5	(8.9)	.018	(0.03)	2.	(40)	.20	(840)
Concrete block	7.6	(19.0)	.50	(0.87)	130.	(2080)	.18	(750)
Plaster	0.7	(1.9)	.42	(0.73)	116.	(1860)	.20	(840)
Roof panels	8.0	(20.0)	.52	(0.90)	85.	(1400)	.20	(840)
Roof pavers	2.0	(5.1)	.43	(0.74)	95.	(1500)	.20	(840)
Quarry tile	0.5	(1.3)	.80	(1.40)	95.	(1500)	.20	(840)
Concrete floor	5.0	(13.0)	.80	(1.40)	150.	(2400)	.20	(840)

* Values taken from refs. 4,5, and 8.

The tracer gas technique was used to determine the air infiltration rate for the test building. A complete description of this technique is given in Appendix B. These measurements revealed that the test building had an extremely low rate of air infiltration. This was attributed to the tight construction and design of the test building. It was shown that air infiltration during winter could be correlated with respect to the inside-to-outside temperature difference. Under these simulated winter conditions, the rate of air infiltration varied from 0.017 to 0.052 volume changes per hour over a range of inside-to-outside temperature differences from 0 to 70 °F (0 to 39 °C). For the summer measurements, the infiltration rate remained essentially constant at about 0.022 volume changes per hour.

For the determination of sol-air temperatures, the surface absorptance of the exterior surface of the test building was taken to be 0.3, and the overall heat-transfer coefficient at the exterior surface was taken to be 1.46 Btu/hr·ft^2·°F (8.24 W/m^2·K). The surface areas used for this analysis were the values given in table 2.

Table 2. SURFACE AREAS USED FOR THE ANALYSIS

Surface	Area	
	ft^2	(m^2)
North wall	260.	(24.1)
East wall	294.	(27.3)
South wall	260.	(24.2)
West wall	273.	(25.4)
Roof	370.	(34.4)
Floor	370.	(34.4)
Window	53.	(4.9)
Door	20.	(1.9)

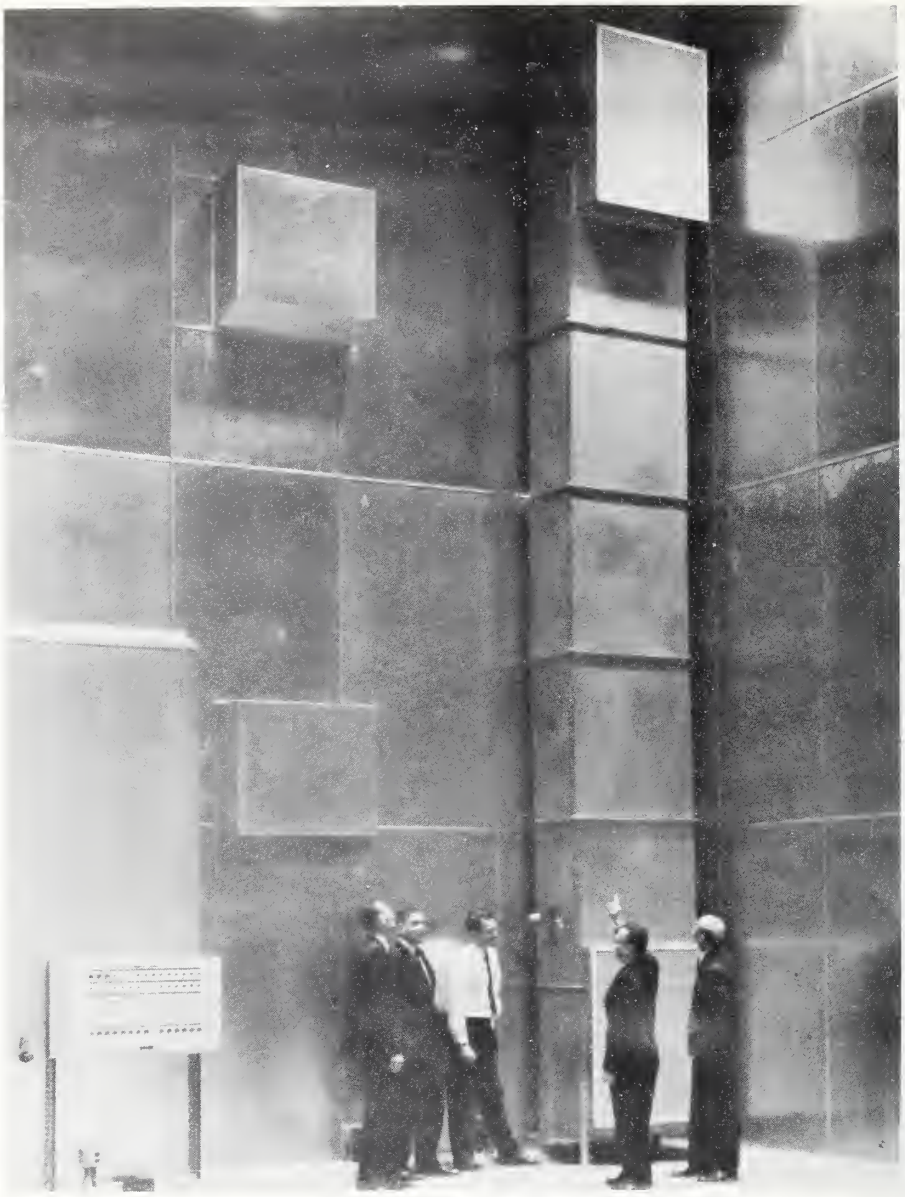

6. EXPERIMENT PLAN

Four tests were carried out in the environmental chamber (see above photograph) and are described in this section. For these tests, the test building was exposed to a diurnal sol-air temperature cycle until a steady-periodic condition was attained. This condition was deemed to exist when the interior temperature fluctuations at various locations repeated themselves at 24-hour intervals.

Nine-hour night cooling test (Test 1): For the 9-hour night cooling test, the test building was repeatedly exposed to a sol-air temperature cycle developed for a peak summer day in Saudi Arabia until the heat flows reached a steady-periodic condition. Hourly values for the sol-air temperature cycle are given in table 3. During this diurnal cycle, the test building was cooled using the valance cooling coil for 9 hours at night,

Table 3. HOURLY SOL-AIR TEMPERATURES, °F (°C)

Time, h	Tests 1 and 2	Test 3	Test 4
0100	79. (26.)	71. (22.)	20. (–6.7)
0200	78. (26.)	70. (21.)	19. (–7.2)
0300	77. (25.)	69. (21.)	18. (–7.8)
0400	76. (24.)	68. (20.)	18. (–7.8)
0500	75. (24.)	68. (20.)	18. (–7.8)
0600	81. (27.)	69. (21.)	18. (–7.8)
0700	95. (35.)	75. (24.)	19. (–7.2)
0800	105. (41.)	91. (33.)	25. (–3.9)
0900	113. (45.)	100. (38.)	33. (–.6)
1000	120. (49.)	107. (42.)	38. (3.3)
1100	125. (52.)	110. (43.)	40. (4.4)
1200	129. (54.)	114. (46.)	42. (5.6)
1300	134. (57.)	119. (48.)	44. (6.7)
1400	136. (58.)	120. (49.)	45. (7.2)
1500	135. (57.)	118. (48.)	43. (6.1)
1600	129. (54.)	110. (43.)	37. (2.8)
1700	120. (49.)	95. (35.)	30. (–1.1)
1800	104. (40.)	88. (31.)	29. (–1.7)
1900	96. (36.)	85. (29.)	27. (–2.8)
2000	92. (33.)	81. (27.)	25. (–3.9)
2100	88. (31.)	78. (26.)	24. (–4.4)
2200	85. (29.)	76. (24.)	22. (–5.6)
2300	83. (28.)	74. (23.)	21. (–6.1)
2400	81. (27.)	73. (23.)	20. (–6.7)

2100 to 0600. The thermostat was set at a low value so that the valance coil operated continuously during the 9-hour period. An internal load was simulated using incandescent light bulbs controlled by a 24-hour clock timer. This internal load was set at 1000 Btu/hr (290 W) from 1900 through midnight and at 500 Btu/hr (146 W) from 0100 until 0700. These loads were selected to simulate the sensible heat released from two dormitory occupants and associated lighting.

Twelve-hour night cooling test (Test 2): For the 12-hour night cooling test, the test building was repeatedly exposed to the same hourly sol-air temperature cycle and internal load schedule as for the previous test. During this test, the valance coil was operated during a 12-hour period from 1800 to 0600. The thermostat was set as 74 °F (23 °C), allowing the valance cooling system to cycle during the night hours.

Night ventilation cooling test (Test 3): For the night ventilation cooling test, the test building was exposed to a reduced diurnal sol-air temperature cycle and the internal load schedule as for the previous two tests. Hourly values of the sol-air temperature cycle are given in table 3. It represents an average November day in Saudi Arabia. Night sky radiation losses were not taken into account in the derivation of this cycle, since they would reduce the night air temperature a few degrees, and thereby affect the ventilation response of the test building. During this cycle, the test building was naturally ventilated during periods when the outdoor air temperature fell below the indoor temperature (i.e., the windows and door were opened and the ceiling fan was operated). The test building was closed in the morning when the simulated outdoor temperature rose above the indoor temperature.

Passive solar test (Test 4): For the passive solar heating test, the test building was exposed to a sol-air temperature cycle representative of an average December day in a mid-western U.S. climate (see table 3). For this cycle, an hourly solar window heat gain for a theoretical clear-sky 40° latitude location [5] in the month of December was simulated using infrared heat lamps. Solar window heat gains used for this test are summarized in table 4. This simulated solar heat gain is equivalent to the theoretical solar heat gain that would enter the test building if all the double-pane window systems were south-facing. The hourly heat output of the infrared heat lamps was adjusted using a variable voltage transformer and measured using a watthour meter. The actual heat output deviated slightly from the theoretical values due to changes in the lamp resistance and experimental error. For the passive solar test, using data contained in ref. [7], a diurnal schedule of internal heat gains was devised to simulate the heat release for lighting, equipment, and occupants for a residence. The test building was assumed to be occupied by two persons during the night and by a single person during the day. The occupancy heat input to the test building was not varied on an hourly basis; rather, the day was divided into two periods and the simulated heat gain was maintained constant during each period. During the daytime period from 0600 to 2100 hours, the simulated occupancy load was maintained at 1470 Btu/hr (430 W). At night from 2100 to 0600 hours, the simulated occupancy load was maintained at 550 Btu/hr (160 W).

Table 4. SOLAR WINDOW HEAT GAINS

Time, h	Heat Gains	
	Btu/hr	(W)
0800-0900	1,870.	(548.)
0900-1000	4,550.	(1,330.)
1000-1100	7,700.	(2,260.)
1100-1200	10,200.	(2,990.)
1200-1300	10,900.	(2,990.)
1300-1400	11,000.	(3,220.)
1400-1500	9,950.	(2,920.)
1500-1600	7,250.	(2,120.)
1600-1700	4,310.	(1,260.)
1700-0800	0	(0)

As in the previous test, the test building was repeatedly exposed to a series of sol-air temperature cycles. The solar window and occupancy heat gains were simulated as described above. After a steady-periodic condition was reached, the indoor temperature response of the test building was recorded.

7. TEST RESULTS

7.1 NINE-HOUR NIGHT COOLING TEST

For the 9-hour night cooling test, a steady-periodic condition was attained in four weeks. A comparison of the predicted and measured indoor air temperatures is given in figure 4. The measured values are the average of the four thermocouple temperatures located along the vertical column. The predicted curve was generated by inputting into the mathematical model hourly measured values for the sensible heat removed by the valance cooling coil. It can be seen that there is good agreement between the measured and corresponding values predicted with the mathematical model, supporting the validity of the model. It should be pointed out that previous studies [4] have shown that inputting indoor temperatures and predicting cooling loads result in much less agreement.

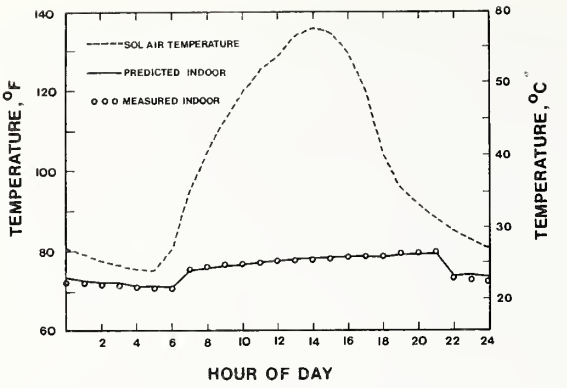

FIGURE 4. COMPARISON OF MEASURED AND PREDICTED INDOOR TEMPERATURES FOR THE 9-HOUR NIGHT COOLING TEST

The hourly sensible loads for the cooling coil were determined by subtracting the latent cooling load from the total cooling load of the coil determined from eq (1). During the operation of the cooling coil, it was not possible to accurately measure the hourly latent load because water tended to accumulate on the fins of the coil until it became saturated and did not readily drain into the condensate collection system. During the first hour of operation of the valance coil, the indoor relative humidity dropped considerably (see fig. 5). For the first hour (2100 to 2200 hours) the latent load (q_1) was estimated from the relation:

$$q_1 = V \cdot \rho \cdot h_{fg} \cdot \Delta\omega_i \qquad (9)$$

where

V = volume of test building;
ρ = density of air;
h_{fg} = latent heat of vaporization; and
$\Delta\omega_i$ = change in humidity ratio of indoor air.

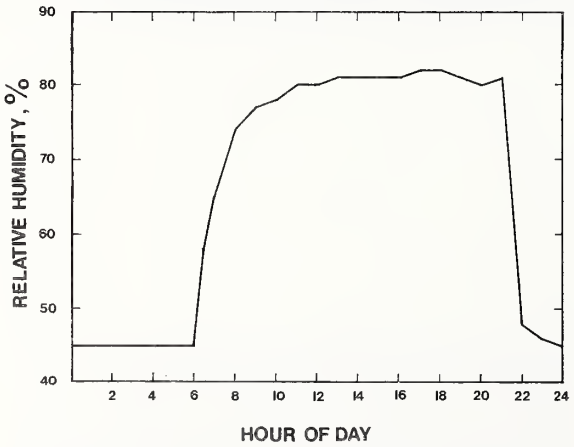

FIGURE 5. VARIATION OF INDOOR RELATIVE HUMIDITY OVER A 24-HOUR PERIOD FOR THE 9-HOUR NIGHT COOLING TEST

For the remaining hours of operation of the valance coil, the latent load (q_l) was estimated from the relation:

$$q_1 = (W - V \cdot \rho \cdot \Delta\omega_i) \cdot h_{fg}/(N-1) \qquad (10)$$

where

W = net condensate collected over a period of a day; and
N = number of hours of coil operation

The other symbols are as previously defined. Here the estimated water collected during the first hour is subtracted from net amount collected during a day. This difference is assumed to condense equally during the remaining operating period of the coil. This is a good assumption, since the indoor relative humidity remained approximately constant during the remaining operating period of the coil (see fig. 5).

For the 9-hour night cooling test, the total amount of condensate collected (W) during the diurnal cycle was 4.8 lb (2.2 kg). The resulting hourly sensible and latent cooling loads determined for the first test are given in table 5. Note that the latent loads are small in comparison with the sensible loads, except during the first hour of coil operation.

When the flow of chilled water ceased, the valance coil remained saturated with water during the period when the cooling system was off, indicating that little water was evaporating from the coil. However, during this same period the indoor relative humidity rose rapidly, suggesting that an additional source of moisture was present. It was hypothesized that the source of this moisture was the wall surface (i.e., original water contained in the concrete mortar holding the concrete blocks together). To verify this hypothesis, a polystyrene container, measuring 17×17×23 in (43×43×58 cm), was sealed to the wall surface. The relative humidity within this container tended to track the rise in indoor relative humidity. This would suggest that the source of moisture was indeed the wall surface. A detailed analysis of wall moisture contribution to the humidity response of the test building is given in Appendix C.

Figure 6 shows the temperatures measured at different heights within the test building. The vertical temperature gradient is observed to be greatest during the system-on hours. However, the gradient is less than 2 °F (1 °C) at all hours of the diurnal cycle. It is interesting to note that during the daytime hours the

Table 5. HOURLY SENSIBLE AND LATENT COOLING LOADS REMOVED BY THE VALANCE COIL FOR 9-HOUR NIGHT COOLING TEST, BTU/HR (W)

Time, h	Sensible		Latent		Total		Latent fraction
	Btu/hr	(W)	Btu/hr	(W)	Btu/hr	(W)	%
2100-2200	9300.	(2700.)	2700.	(790.)	12,000.	(3,520.)	23.
2200-2300	8700.	(2500.)	310.	(91.)	9,010.	(2,640.)	3.
2300-2400	8400.	(2500.)	310.	(91.)	8,710.	(2,550.)	4.
2400-0100	8100.	(2400.)	310.	(91.)	8,410.	(2,460.)	4.
0100-0200	8000.	(2300.)	310.	(91.)	8,310.	(2,430.)	4.
0200-0300	7800.	(2300.)	310.	(91.)	8,100.	(2,380.)	4.
0300-0400	7800.	(2300.)	310.	(91.)	8,110.	(2,380.)	4.
0400-0500	7700.	(2300.)	310.	(91.)	8,010.	(2,350.)	4.
0500-0600	7700.	(2300.)	310.	(91.)	8,010.	(2,350.)	4.
0600-2100	0.	(0)	0.	(0)	0.	(0)	-

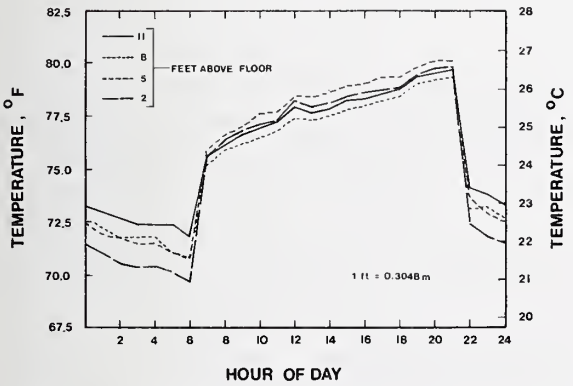

FIGURE 6. MEASURED INDOOR TEMPERATURES AT VARIOUS HEIGHTS

floor-to-ceiling temperature gradient is less than 1 °F (0.6 °C). These results support the validity of the assumption that the indoor air is perfectly mixed (see sec. 4).

The foregoing results indicated that the operation of the valance cooling coil only during a 9-hour night period to cool interior mass of the walls, ceiling, and floor resulted in an adequate indoor temperature during the day period. The observed daytime temperature rise of 6 °F (3.3 °C) is acceptable, although during this 15-hour period the relative humidity rose to 80 percent. The source of moisture was determined to be primarily from the masonry surfaces of the test building. This condition was attributed to the original water contained in the concrete mortar.

The sol-air diurnal temperature cycle used for the 9-hour night cooling test was derived from weather data for a desert climate. It is based upon a daytime high temperature of 110 °F (43.3 °C) and nighttime low temperature of 79 °F (26 °C). This temperature cycle is seen to be hotter than all the selected cities of the the United States shown in table 6. It should be noted that certain remote desert regions within the United States may exhibit temperature extremes which exceed the simulated diurnal temperature cycle. It is therefore apparent that night mechanical cooling of a building of this type construction is a viable strategy for all habitable locations of the United States.

7.2 TWELVE-HOUR NIGHT COOLING TEST

For the 12-hour night cooling test, the measured and predicted indoor temperatures are compared in figure 7. The variation in indoor temperature was similar to that found in the previous test. Good agreement was again observed between predicted and measured

Table 6. THE NORMAL DAILY AIR TEMPERATURE EXTREMES AND RELATIVE HUMIDITIES FOR SELECTED CITIES FOR JULY

	High °F(°C)	Low °F(°C)	RH%	At time
Albuquerque	91 (33)	66 (19)	36	1100
Atlanta	87 (31)	71 (22)	64	1300
Chicago	81 (27)	67 (19)	55	1200
Dallas	95 (35)	75 (24)	50	1200
Denver	88 (31)	57 (14)	36	1300
Houston	94 (34)	71 (22)	55	1200
Los Angeles	76 (24)	62 (17)	68	1000
Memphis	91 (33)	72 (22)	57	1200
Miami	89 (32)	75 (24)	64	1300
Minneapolis	84 (29)	61 (16)	56	1200
Nashville	91 (33)	70 (21)	58	1200
New York	85 (29)	68 (20)	55	1300
Omaha	90 (32)	67 (19)	45	1100
Pheonix	105 (41)	75 (24)	29	1100
Pittsburgh	85 (29)	65 (18)	--	--
San Francisco	64 (18)	53 (12)	75	1000
Seattle	76 (24)	54 (12)	66	1000
St. Louis	89 (32)	67 (19)	58	1200
Washington, DC	87 (31)	69 (21)	52	1300

indoor temperatures. For this test, the thermostat was set at 74 °F (23 °C), and the indoor temperature rose 7 °F (4 °C) during the 12-hour daytime period when the valance coil was not operated.

The measured values in figure 7 are the average of the four sensors located on the vertical column time averaged during each hour. The time averaging was necessary because the cyclic operation of the valance coil produced fluctuations in indoor temperature.

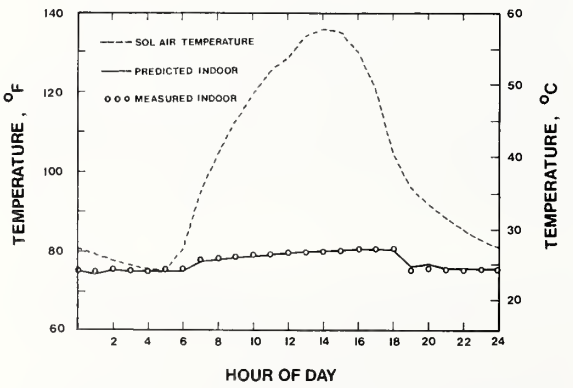

FIGURE 7. COMPARISON OF MEASURED AND PREDICTED INDOOR TEMPERATURE FOR THE 12-HOUR NIGHT-COOLING TEST

As in the case for the previous test, the predicted indoor temperature was obtained by inputting hourly values of the sensible cooling load into the mathematical model (see table 7) during the night hours.

For the 12-hour night cooling test, 3.3 lb (1.5 kg) of water was collected each day, and a similar trend in relative humidity to that observed during the first test was observed for the 12-hour night cooling test.

At the conclusion of this test, the sol-air cycle in the environmental chamber was continued, and the valance cooling was stopped. Unfortunately, a malfunction of the environmental chamber permitted only 30 hours of data to be recorded.

The recorded results along with corresponding values predicted with the mathematical model for 50-hours are shown in figure 8. It is seen that the measured indoor temperatures closely followed the predicted values. It is interesting to note the slow rate at which the indoor air temperature rose. After 30 hours, the indoor temperature rose only 10 °F (5.6 °C), including the 6 °F (3 °C) rise which occurred during the first hour when the valance cooling system was shut off.

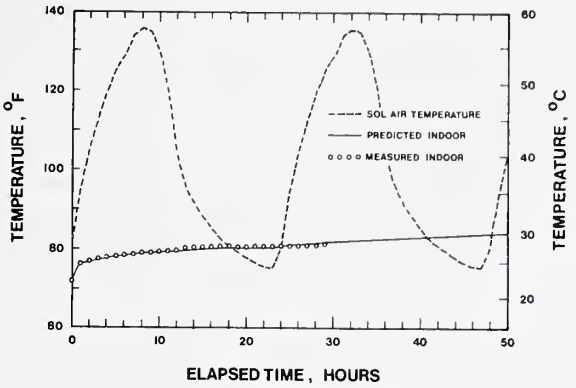

FIGURE 8. COMPARISON OF MEASURED AND PREDICTED INDOOR TEMPERATURES AFTER THE VALANCE COOLING WAS STOPPED FOLLOWING THE 12-HOUR NIGHT-COOLING TEST

Table 7. HOURLY SENSIBLE AND LATENT COOLING LOADS REMOVED BY VALANCE COIL FOR 12-HOUR NIGHT COOLING TEST, BTU/HR (W)

Time, h	Sensible Btu/hr (W)	Latent Btu/hr (W)	Total Btu/hr (W)	Latent Fraction %
1800-1900	8,800. (2,600.)	2,700. (790.)	11,500. (3,370.)	23
1900-2000	6,000. (1,800.)	140. (41.)	6,140. (1,800.)	2
2000-2100	7,600. (2,200.)	140. (41.)	7,740. (2,270.)	2
2100-2200	6,900. (2,000.)	140. (41.)	7,040. (2,060.)	2
2200-2300	6,500. (1,900.)	140. (41.)	6,640. (1,950.)	2
2300-2400	6,200. (1,800.)	140. (41.)	6,340. (1,860.)	2
2400-0100	4,800. (1,400.)	140. (41.)	4,940. (1,450.)	3
0100-0200	4,400. (1,300.)	140. (41.)	4,540. (1,330.)	3
0200-0300	4,900. (1,400.)	140. (41.)	5,040. (1,470.)	3
0300-0400	4,400. (1,300.)	140. (41.)	4,540. (1,330.)	3
0400-0500	4,400. (1,300.)	140. (41.)	4,540. (1,330.)	3
0500-0600	4,300. (1,300.)	140. (41.)	4,440. (1,300.)	3

7.3 NIGHT VENTILATION COOLING TEST

For the night ventilation cooling test, the ventilation rate during periods of night ventilation was determined using the tracer-gas technique (see Appendix B), and found to be approximately 14 volume changes per hour. The measured and predicted indoor temperatures for this test are compared in figure 9. The mathematical model closely predicted the indoor temperature during all parts of the diurnal cycle.

It is seen from figure 9 that the indoor temperature remained below 79 °F (26 °C), even though the valance cooling system was not operated. The mathematical model was used to predict the total cooling load that would be required to maintain the test building at 79 °F (26 °C) if it were air conditioned in a conventional manner. The predicted total cooling load was 36,000 Btu (10,500 W·hr) for the sol-air cycle shown in figure 9. This is the amount of energy that is saved by the night ventilation cooling.

The chamber dewpoint temperature for this test was maintained at a constant value of 54 °F (12 °C). This value is the average dewpoint temperature for Makkah in November, as derived from site weather data. The use of night ventilation alleviated the humidity problem previously discussed. The night air was observed to dry the wall surfaces sufficiently to maintain the relative humidity level below 50 percent during daytime periods.

During this test, an investigation was made to determine the recovery time for the test building when it was exposed to brief periods of infiltration during the hot part of the day. This gave an indication of the rate at which cool interior mass of the walls, roof, and floor absorbs heat. During the hottest period of the day, the windows and doors of the test building were opened and the ceiling fan was turned on, ventilating the test building with approximately 14 volume changes per hour at an outdoor temperature of 120 °F (49 °C). This ventilation rate was continued for approximately 8 minutes until the indoor temperature tended to level off (see fig. 10). At this time, the rate of heat absorption by the walls is approximately balanced by the energy added by infiltrating air. The test building was subsequently closed off and the indoor temperature response was recorded. From figure 10, it is seen that the indoor temperature of the test building recovered within 10 minutes with cooling being provided solely by the interior building mass.

For the night ventilation cooling test, the measured indoor air temperature remained below 79 °F (26 °C) without mechanical cooling. The sol-air temperature cycle used for the night ventilation test was based on an outdoor air temperature that ranged from a daytime high of 93 °F (34 °C) to a nighttime low of 68 °F (20 °C). Most regions of the United States exhibit similar, or lower, temperature extremes for their peak summer months (see table 6). Therefore, it is apparent that night ventilation is a viable cooling strategy for this type of construction in most parts of the United States.

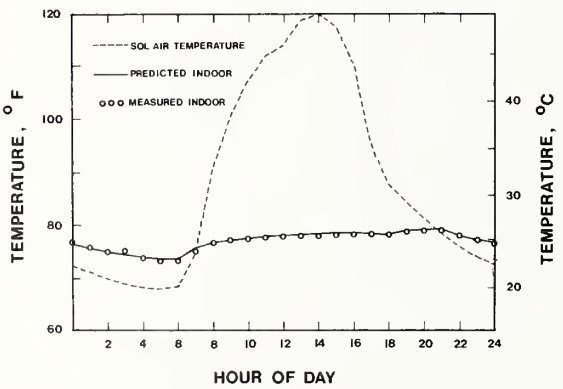

FIGURE 9. COMPARISON OF MEASURED AND PREDICTED INDOOR TEMPERATURES FOR THE NIGHT VENTILATION COOLING TEST

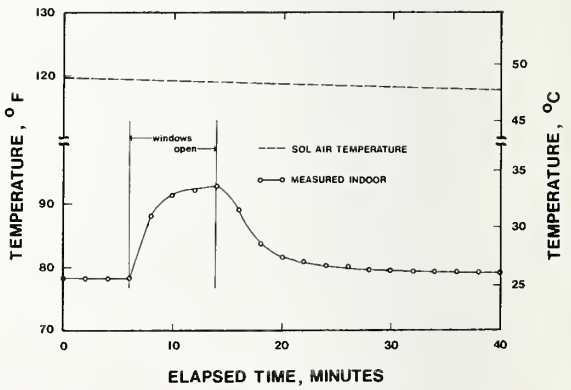

FIGURE 10. RESPONSE OF THE INDOOR TEMPERATURE TO A BRIEF PERIOD OF VENTILATION DURING THE HOT PART OF THE DAY

7.4 PASSIVE SOLAR HEATING TEST

For the passive solar heating test, the measured and predicted indoor temperature responses for the test building are compared in figure 11. It is seen that a near-comfort condition was maintained even with the small amount of simulated window solar heat gain (i.e., 21 percent glass in south wall). The agreement between the measured and predicted values is good.

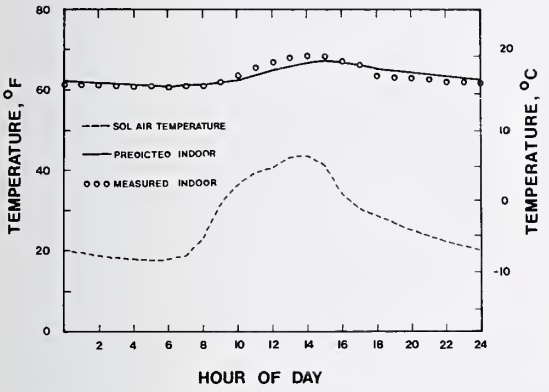

FIGURE 11. COMPARISON OF MEASURED AND PREDICTED INDOOR TEMPERATURE RESPONSE OF THE TEST BUILDING FOR THE PASSIVE SOLAR TEST

8. SUMMARY AND CONCLUSIONS

A well-insulated test building having high interior mass was constructed within a high-bay environmental chamber at the National Bureau of Standards. This test building was subjected to a series of diurnal sol-air temperature cycles, and the indoor temperature response of this building was measured when the following three energy-conservation schemes were implemented: night cooling using a ceiling-mounted chilled-water valance coil; night ventilation cooling; and passive solar heating. For a 9-hour night cooling test, the valance cooling coil system of the test building was operated continuously during a 9-hour night period. During the 15-hour day period, the indoor temperature was observed to rise only 6 °F (3.3 °C). However, the indoor relative humidity rose to 80 percent during the same period. The source of this moisture was determined to be primarily from the masonry surfaces. This condition was attributed to the original water contained in the concrete mortar during its construction.

A similar test, using a 12-hour night cooling period, was carried out. During this test, the operation of the valance cooling coil system was thermostated and maintained the indoor temperature at an average value of 74 °F (23 °C). For this test, the indoor temperature rose 7 °F (4 °C) during the 12-hour daytime period when the valance cooling coil was not operated.

The diurnal sol-air temperature cycle used for the night cooling tests was derived from weather data for a desert climate which is hotter than all habitable parts of the United States. It is therefore apparent that night mechanical cooling of a building of this type construction is a viable strategy for all habitable locations of the United States.

For the night ventilation cooling test, the test building was exposed to a sol-air temperature cycle having a daytime high of 93 °F (34 °C) and a nighttime low of 68 °F (20 °C). The test building was naturally ventilated by opening the windows and operating a ceiling fan during periods when the outdoor temperature fell below the indoor temperature. During the day period when the test building was closed, the indoor temperature remained below 79 °F (26 °C) without mechanical cooling. Most regions of the United States are seen to exhibit similar temperature extremes for their peak summer months. Therefore, it is apparent that night ventilation is an energy saving cooling strategy for buildings having this type construction in most parts of the United States.

For the passive solar heating test, the test building was exposed to a diurnal sol-air temperature cycle representative of an average December day in a mid-western climate. During this test, an hourly (clear day) solar window heat gain for 21 percent glass in the south wall was simulated using infrared heat lamps. A near comfort indoor condition was maintained even with the small amount of simulated solar window gain.

REFERENCES

1. "Analytical Study for Building Construction Parameters on Dynamic Response for Intermittent System Operation and Outdoor Ventilation." Technical Report No. SOM-ME-78-1, Skidmore, Owings and Merrill, Chicago, January 1978.
2. "Procedure for Determining Heating and Cooling Loads for Computerized Energy Calculations," Algorithms for Building Heat Transfer Subroutines, ASHRAE Task Group, 1976.
3. Mitalas, G. P. and Arsenault, J. G., "Fortran IV Program to Calculate z-transfer Functions for the Calculation of Transient Heat Transfer through Walls and Roofs," DBR Computer Program No. 33, Ottawa, Canada, June 1972.
4. Peavy, B. A., Powell, F. J., and Burch, D. M., "Dynamic Thermal Performance of an Experimental Masonry Building," National Bureau of Standards Building Science Series 45, July 1973.
5. *ASHRAE Handbook of Fundamentals*, American Society of Heating, Refrigerating and Air Conditioning Engineers, 1977.
6. Peavy, B. A., Burch, D. M., Powell, F. J., and Hunt, C. M., "Comparison of Measured and Computer-Predicted Thermal Performance of a Four-Bedroom Wood-Frame Townhouse," National Bureau of Standards Building Science Series 57, April 1975.
7. "Mixed Strategies for Energy Conservation and Alternative Energy Utilization (Solar) in Buildings," Energy Resources Center, Honeywell, Inc., Minneapolis, Minn., 1978.
8. Kreith, F., *Principles of Heat Transfer*, Second Edition, International Textbook Co., Scranton, Pa., 1965.
9. Burch, D. M. and Hunt, C. M., "Retrofitting an Existing Wood-Frame Residence for Energy Conservation—An Experimental Study," National Bureau of Standards Building Science Series 105, July 1978.
10. Hunt, C. M. and Burch, D. M., "Air-Infiltration Measurements in a Four Bedroom Townhouse Using Sulfur Hexafluoride as a Tracer Gas," ASHRAE Transactions 81, Part 1, p. 186-201, 1975.

APPENDIX A

THERMOGRAPHIC SURVEY

S. J. Treado

A method for investigating the thermal performance of buildings and their components is infrared thermography. An infrared television system senses the long-wave radiation emitted and reflected from a surface. This radiation is received by an infrared camera and converted into a video signal which is displayed on a color or black-and-white oscilloscope monitor. For the color monitor, the surface temperatures are represented by 10 color-coded isotherms. The temperature difference between adjacent isotherm units is dependent on a sensitivity setting of the equipment. A conventional camera is used to photograph the oscilloscope screen. A photograph of the oscilloscope screen is called a thermogram. A more detailed description of thermographic equipment and measurement technique is given in ref. [9].

The experiment procedure followed in carrying out the thermographic survey was to expose the test building for several days to the diurnal cycle for tests 1 and 2. At the time of the survey, the indoor temperature was approximately 75 °F (24 °C) and the outdoor temperature approximately 120 °F (49 °C).

Each figure contains two photographs. The first shows a part of the building in the visible spectrum; the second is a thermogram which is a thermal picture of the scene as viewed by the IR camera. The sensitivity of the system was adjusted such that the temperature range displayed in the thermal picture was 9 °F (5 °C). Therefore, each of the 10 colors displayed in the thermal picture represents approximately a 0.9 °F (0.50 °C) temperature band. The temperature ascends from cold to hot, correspondingly left to right on the scale displayed at the bottom. The relative surface temperature between different surfaces displayed in the thermal picture may be determined by comparing the color of the locations with the color scale displayed at the bottom.

The first surface to be viewed was an external corner of the test building (see fig. A.1). A vertical temperature gradient is shown along the wall surface from the floor to the ceiling. This is shown by the change from dark blue near the ground to the beginning of red-purple on the wall near the top edge of the window. This corresponds to a change of five color isotherms on the scale, or a temperature change of 4.5 °F (2.5 °C). The infrared picture was taken during the initial conditioning period before the test building reached a steady-periodic condition.

FIGURE A.1 (a). CONVENTIONAL PHOTOGRAPH OF THE TEST HOUSE

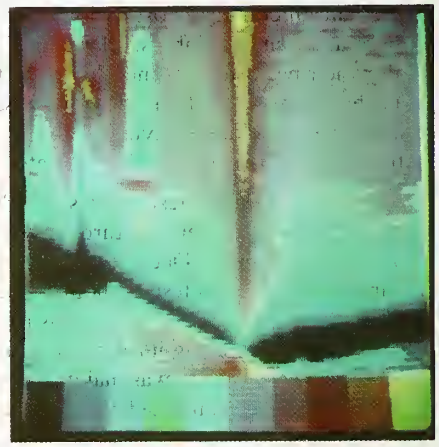

FIGURE A.1 (b). INFRARED PHOTOGRAPH OF THE TEST HOUSE

Thermograms taken after a steady-periodic condition was reached showed that vertical temperature gradients did not exist within the test building. The relatively warm region at the corner is due to two-dimensional heat transfer.

Figure A.2 shows an upper inside corner of the test building. A thermal bridge is observed in this region. Inspection of the construction of the test building in the vicinity of the thermal bridge revealed a high-conductance heat-flow path which by-passed the insulation. The higher heat transmission through this

FIGURE A.2 (a). CONVENTIONAL PHOTOGRAPH OF THE UPPER INSIDE CORNER

FIGURE A.3 (a). CONVENTIONAL PHOTOGRAPH OF THE INSIDE DOOR SURFACE

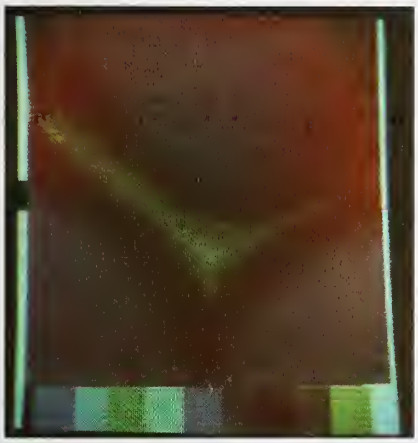

FIGURE A.2 (b). INFRARED PHOTOGRAPH OF THE UPPER INSIDE CORNER

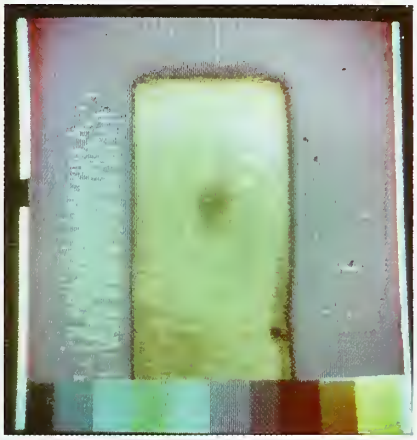

FIGURE A.3 (b). INFRARED PHOTOGRAPH OF INSIDE DOOR SURFACE

part is displayed in tan and red. This effect weakens the validity of the assumption that the heat transfer is one-dimensional (see sec. 4.1). The impact of this defect and others on the overall performance of the test building was assumed to be small. Therefore, these defects were not corrected. Figure A.3 shows the interior door surface of the test building. The door is observed to be warmer than the wall surfaces, indicating a relatively larger heat flow through this region. It is interesting to note that the doorknob appears cooler. However, the doorknob has a lower emittance than other building surfaces displayed in the thermal picture, causing it to appear colder than other surfaces. The cooler spot in the center of the door is caused by the insulating effect of a small sign hanging on the exterior surface of the door.

The valance coil in operation is shown in figure A.4. The coil is observed to create a low-temperature region along the rear wall extending 3 to 4 feet below the coil. This is caused by the cool valance discharge air scrubbing the wall surface. Also seen in this

FIGURE A.4 (a). CONVENTIONAL PHOTOGRAPH OF VALANCE COIL

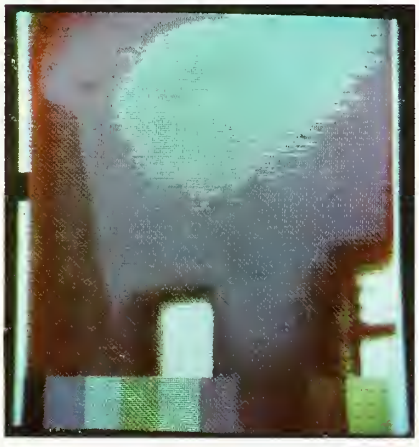

FIGURE A.4 (b). INFRARED PHOTOGRAPH OF VALANCE COIL

thermogram is a large temperature difference between the wall and the window frame (blue to yellow on the isotherm scale).

The thermographic system was also used to investigate the air leakage paths of the test building. For these measurements, a blower was utilized to depressurize the building, and the thermographic system was used to detect warmer regions heated by infiltrating air. The region of most pronounced air infiltration was observed at the interface of the wall and ceiling. This air leakage path can readily be seen in figure A.5.

In summary, the bulk of the wall areas appeared to be at a uniform temperature, except for a few areas, indicating that the test building was essentially free of thermal bridges.

FIGURE A.5 (a). CONVENTIONAL PHOTOGRAPH OF WALL/CEILING EDGE

FIGURE A.5 (b). INFRARED PHOTOGRAPH OF WALL/CEILING EDGE

APPENDIX B

AIR INFILTRATION MEASUREMENTS

Robert M. Caravello

B.1 THEORY

A small amount of tracer gas, sulfur hexafluoride (SF_6), was released within the test building and the tracer gas concentration was measured as a function of time over a 10-hour period as it decayed. During these measurements, the indoor temperature was maintained at 75 °F (24 °C). Mixing was achieved by using the overhead fan. The decay of tracer gas was caused by air infiltration.

For a first-order exponential decay process, the change in tracer concentration with respect to time is given by the relation:

$$-\frac{dc}{dt} = \frac{v}{V} \cdot c \qquad \text{(B-1)}$$

where

c = concentration of tracer gas, ppb;
v = air infiltration rate, ft^3/hr (m^3/s);
V = volume of the test building, ft^3 (m^3); and
t = time, hr (s).

For an initial concentration of c_o, the solution to eq (B-1) is given by

$$c = c_o \cdot e^{-(v \cdot t/V)} \qquad \text{(B-2)}$$

or

$$I = \frac{v}{V} = -\frac{1}{t} \ln(c/c_o)$$

where

I = air infiltration rate, volume change/hr; and
c_o = initial concentration at t=0, ppb.

The foregoing expression was used to determine the air infiltration rate (I) from measured time decaying values of the SF_6 concentration.

B.2 MEASUREMENT TECHNIQUE

Sulfur-hexafluoride (SF_6) concentrations were measured with a gas chromatograph equipped with an electron-capture detector. Sampling and analysis were performed semi-automatically. The logarithm of the relative concentration (c/c_o) was was plotted as a function of time. A best-fit straight line was obtained using a least-squares procedure. The negative slope of this straight line was taken to be equal to the rate of air infiltration.

Further information on the SF_6 tracer-gas technique may be found in ref. [10].

B.3 RESULTS

Table B.1 gives the measured infiltration rates for the test building when the indoor temperature was maintained at a constant 75 °F (24 °C) and the outdoor temperature was maintained constant at five different conditions.

Table B.1. MEASURED RATES OF AIR INFILTRATION

Infiltration Rate, volume changes per hour	ΔT °F	ΔT °C	Condition
.033	40.	22	Winter
.052	70.	39	Winter
.017	0.	0	No temp. diff.
.022	-20.	-11	Summer
.022	-40.	-22	Summer

The winter values given in table B.1 were fitted to the following linear expression:

$$I = A + B \cdot (T_i - T_o) \qquad \text{(B-3)}$$

Here A and B are constants. A regression analysis gave the following correlation:

$$I = 0.0159 + 0.000495 \cdot (T_i - T_o) \qquad \text{(B-4)}$$

A plot of the infiltration rate as a function of temperature difference is given in figure B.1. With a temperature difference ($T_i - T_o$) equal to 0 °F (0 °C), the infiltration rate was 0.017 volume changes per hour.

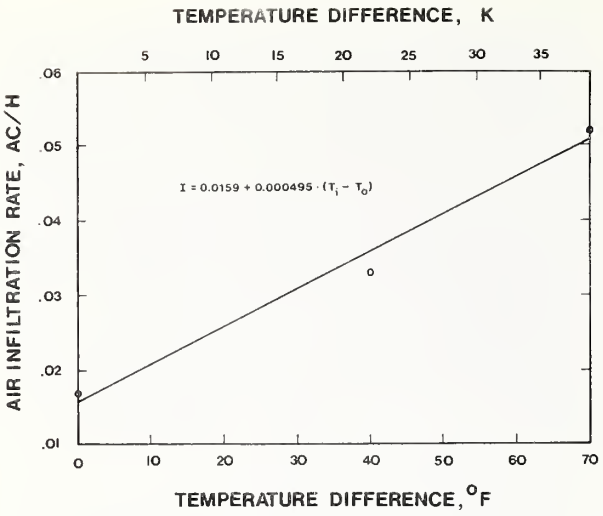

FIGURE B.1. RATE OF AIR INFILTRATION PLOTTED AS A FUNCTION OF THE INSIDE-TO-OUTSIDE TEMPERATURE DIFFERENCE

At a temperature difference of 70 °F (39 °C), the rate of air infiltration was 0.052 volume changes per hour. These figures indicate that the test building has an extremely low rate of air infiltration due to its very tight construction and the use of low-permeability polystyrene insulation in the walls, ceiling, and floor.

It should be noted that in deriving the curve given in figure B.1 only winter values were used. Note that the infiltration rate increased as the temperature difference increased. The two summer measurements were excluded because they did not show a correlation with respect to temperature difference.

Approximately eight door openings occurred during each of the measurements. It is estimated that these door openings contributed approximately 0.0027 volume changes per hour,

B.4 CONCLUSIONS

Air infiltration measurements revealed that the test building possessed extremely tight construction. It was shown that air infiltration during winter could be correlated with respect to the inside-to-outside temperature difference. Under these simulated winter conditions, the rate of air infiltration varied from 0.017 to 0.052 volume changes per hour over a range of inside-to-outside temperature differences from 0 to 70 °F (0 to 39 °C). For the summer measurements, the infiltration rate was observed to remain essentially constant at about 0.022 volume changes per hour.

APPENDIX C

WALL MOISTURE CONTRIBUTION TO THE HUMIDITY RESPONSE OF THE TEST BUILDING

The purpose of this appendix is to present a mathematical model for predicting the indoor humidity response of the test building. It has been noted in the main body of the report that, when a polystyrene container, measuring $17\times17\times23$ in ($43\times43\times58$ cm), was sealed to the interior wall surface, the relative humidity within the container tended to track the rise in indoor relative humidity. This would suggest that the source of moisture that caused the indoor humidity to rise was the wall surface (i.e., the original water contained in the mortar holding the concrete blocks together). For the present analysis, it is assumed that the source of moisture is indeed the wall surface. The analysis is presented herein.

The rate of change of the moisture content of the indoor air is equal to the rate of evaporation from the wall surface, or:

$$\rho V \frac{d\omega}{dt} = h \cdot A \cdot (\omega_{sat}-\omega) \qquad \text{(C-1)}$$

where

ρ = density of indoor air, lb/ft^3 (kg/m^3);
V = inside volume of test building, ft^3 (m^3);
ω = humidity ratio of indoor air, lb water/lb air (kg water/kg air);
h = water-vapor transfer coefficient, lb water/hr·ft^2 (kg water/s·m^2);
ω_{sat} = saturation humidity ratio of interstices of wall surface, lb water/lb air (kg water/kg air);
t = time, hr(s); and
A = surface area of walls, ft^2(m^2);

For this analysis, it is assumed that the water-vapor transfer coefficient (h) and the saturation humidity ratio (ω_{sat}) of the interstices of the wall surface are constant. Separating the variables and applying the initial condition:

$$\omega = \omega_o \text{ at } t = o$$

we obtain the following solution to (C-1):

$$\frac{\omega_{sat}-\omega}{\omega_{sat}-\omega_o} = e^{-t/(\rho V/hA)} \qquad \text{(C-2)}$$

The quantity ($\rho V/hA$) is a time constant for a first-order exponential process.

An average value for the water-vapor transfer coefficient (h) may be obtained by integrating the right side of (C-1) over the period (P) during which the chilled-water coil is operated, or

$$h = \frac{W}{A \int_o^P (\omega_{sat}-\omega)dt} \qquad \text{(C-3)}$$

Here W is the weight of condensate collected over the period P, and the other symbols are as previously defined.

For the first test (9-hour night cooling test), the weight of condensate collected was 4.8 lb (2.2 kg). The temperature of the interstices of the wall was taken to be 75 °F. The saturation humidity ratio corresponding to this temperature is 0.0188 lb water/lb dry air (or 0.0188 kg water/kg dry air). The interior surface area (A) of the walls is 1087 ft^2 (101 m^2). Using measured values for W during the period P, the integral of eq (C-3) was found to be 0.0963 lb water·hr/lb·air. Substituting these quantities into (C-3), the water-vapor transfer coefficient (h) was found to be 0.0459 lb air/hr·ft^2, and the thermal time constant ($\rho V/hA$) was found to be 7.3 hours. Therefore,

$$\frac{\omega_{sat}-\omega}{\omega_{sat}-\omega_o} = e^{-t/7.3} \qquad \text{(C-4)}$$

After the chilled water coil was turned off, the humidity ratio of the indoor air approached the saturation humidity ratio of the interstices of the wall. Therefore, we can divide the numerator and denominator of the left side by ω_{sat} and making use of the approximate relation for relative humidity (ϕ):

$$\phi \simeq \omega/\omega_{sat} \qquad \text{(C-5)}$$

we obtain:

$$\frac{1-\phi}{1-\phi_o} = e^{-t/7.3} \qquad \text{(C-6)}$$

Here ϕ_o is the initial relative humidity.

The predicted humidity response given by equation (C-6) is compared to the measured response during the 15-hour period for test 1 when the chilled-water coil is turned off in figure C.1. Note that the predicted indoor relative humidity rises considerably more slowly than the measured response. This suggests that either there is another source of moisture or that the wall is drying out more rapidly than predicted by the

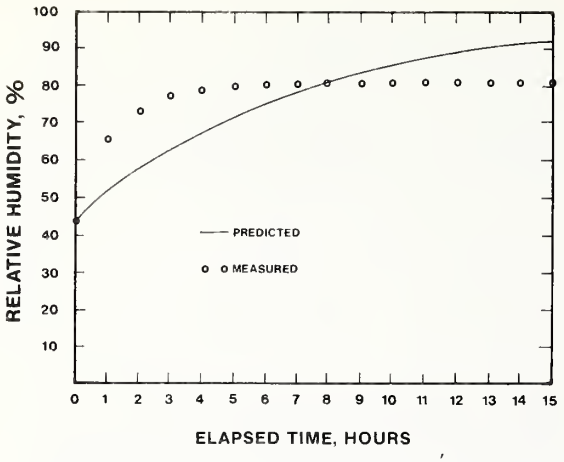

FIGURE C.1. COMPARISON OF MEASURED AND PREDICTED INDOOR RELATIVE HUMIDITY FOR THE PERIOD WHEN THE COOLING COIL IS TURNED OFF

model. During the 15-hour off period, the temperature of the interstices of the wall may increase above 75 °F, giving rise to an increased rate of evaporation of water. The chilled water coil is another source of moisture not accounted for in the model. In addition, the predicted response rises to a higher value than the measured response at the end of the 15-hour period. This is probably because the mathematical model does not account for loss of moisture from the space due to air infiltration.

APPENDIX D

EVALUATION OF THE EFFECT OF ENVIRONMENTAL CHAMBER WALL TEMPERATURE ON THE PERFORMANCE OF THE TEST BUILDING

For the test carried out, the test building was exposed to a sol-air temperature cycle. A sol-air temperature is an equivalent outdoor temperature which produces the same overall rate of heat conduction through the opaque portions of the building envelope as would exist if the test building were exposed to a combined outdoor ambient air and solar load. The test building was located within an environmental chamber, and its exterior surfaces exchange heat not only by means of convection with the ambient air but also by means of radiation with the walls of the environmental chamber. When the temperature of the chamber walls differs from that of the ambient air within the environmental chamber, the building senses an effective sol-air temperature which is different than the desired value. This causes the rate of heat conduction through the building envelope to be different than it would be if the ambient air and chamber walls were at the same temperature.

In this appendix, the effect of radiation exchange between a wall of the test building and the chamber walls on the effective sol-air temperature is analyzed. It is assumed that the results for the entire test building are very similar to the response of a single wall. The analysis is presented herein.

The heat transfer at an exterior surface of the test building is the sum of the convection and radiation exchange, or

$$q_s/A = h_c \cdot (T_{sa}-T_s) + \sigma \cdot F_{12} \cdot [(T_{cw}+460)^4 - (T_s+460)^4] \qquad \text{(D-1)}$$

where

q_s/A = heat transfer at an exterior surface of the test building, Btu/hr·ft^2 (W/ft^2);
h_c = convection heat-transfer coefficient, Btu/hr·ft^2·°F (W/m^2·K);
T_{sa} = sol-air temperature cycle, °F (°C);
T_s = surface temperature of test building, °F (°C);
σ = Stefan-Boltzmann constant, Btu/hr·°F^4 (W/K^4);
F_{12} = configuration factor from surface 1 to 2 with consideration taken for the emittance of the two surfaces; and
T_{cw} = chamber wall temperature, °F (°C).

Treating the two surfaces as parallel flat plates, the gray-body configuration factor is given by the relation:

$$F_{12} = 1/(1/\epsilon_s+1/\epsilon_{cw}-1). \qquad \text{(D-2)}$$

Here the emittance for the test building (ϵ_s) was taken to be 0.93 and emittance for the dull aluminum chamber walls (ϵ_{cw}) was taken to be 0.85 [8].

The heat transfer occurring at the exterior surface from combined radiation and convection is equated to the case where the chamber wall surface temperatures are the same as the sol-air temperature. This is given by the following relation:

$$q_s/A = (h_c+h_r) \cdot (T_e-T_s) \qquad \text{(D-3)}$$

where

q_s/A = defined by eq (D-1);
h_r = radiation coefficient = $4\ \sigma\ F_{12}\ (t_m+460)^3$, Btu/hr·ft^2·°F, (W/m^2·K);
t_m = mean temperature between the exterior of the test building and the chamber walls at the sol-air temperature °F (°C); and
T_e = effective sol-air temperature, °F (°C).

The effective sol-air temperature (T_e) in eq (D-3) represents the equivalent chamber air temperature which produces the same heat exchange that would occur when the ambient and chamber walls are at a different temperature.

The value of T_e was calculated for test 4 from recorded values of all other variables, i.e., T_{sa}, T_s, and T_{cw}. The ambient air and surface temperatures were measured with thermocouples. The chamber wall temperature was taken as the average value of three surface-mounted thermocouples at the chamber wall. The value of h_c was estimated using the relation:

$$h_c = 0.19(\Delta T)^{1/3} \qquad \text{(D-4)}$$

where

ΔT = temperature difference between surface and air, °F.

This expression is applicable to natural convection at a vertical surface. The measured values and the calculated effective sol-air temperatures are given in columns 4 and 5 of table D.1. The effective sol-air temperature represents the temperature felt by the test building through the combined effects of radiation and convection. Ideally, this temperature should equal the sol-air cycle; however, this is not the case. The maximum difference (column 6) between the sol-air

Table D.1. MEASURED TEMPERATURES AND CALCULATED VALUES

Time, h	Chamber wall °F (°C)		Building wall °F (°C)		Sol-air temp. °F (°C)		Effective sol air °F (°C)		ΔT °F (°C)	
0000	27.9	(−2.3)	31.1	(−0.5)	24.0	(−4.4)	25.9	(−3.4)	−1.9	(−1.1)
0200	25.4	(−3.7)	28.7	(−1.8)	21.1	(−6.1)	23.2	(−4.9)	−2.1	(−1.2)
0400	23.5	(−4.7)	26.7	(−2.9)	19.9	(−6.7)	21.7	(−5.7)	−1.8	(−1.0)
0600	21.7	(−5.7)	24.7	(−4.1)	18.0	(−7.8)	19.8	(−6.8)	−1.8	(−1.0)
0800	20.5	(−6.4)	23.9	(−4.5)	19.0	(−6.7)	19.8	(−6.8)	−0.8	(0.4)
1000	27.9	(−2.3)	26.5	(−3.1)	29.5	(−1.4)	28.6	(−1.9)	0.9	(0.5)
1200	35.5	(1.9)	31.0	(−5.6)	37.4	(3.0)	36.4	(2.4)	1.0	(0.6)
1400	41.1	(5.1)	35.4	(1.9)	43.4	(6.3)	42.2	(5.7)	1.2	(0.7)
1600	43.4	(6.3)	38.5	(3.6)	43.6	(6.4)	43.5	(6.4)	0.1	(0.1)
1800	37.9	(3.3)	37.4	(3.0)	33.5	(0.8)	35.9	(2.2)	−2.4	(−1.3)
2000	33.3	(0.7)	35.3	(1.8)	29.0	(−1.7)	31.2	(−.4)	−2.2	(−1.2)
2200	30.7	(−0.7)	33.3	(0.7)	27.0	(−2.8)	28.9	(−1.7)	−1.9	(−1.1)

and effective sol-air temperature is seen to be 2.4 °F (1.3 °C), indicating that the test building feels the actual sol-air temperature to within 2.4 °F (1.3 °C) throughout the diurnal cycle. This deviation is small compared with the temperature difference across the envelope of the test building. Therefore, the effect of radiation exchange between the test building and the chamber walls on the heat conduction through the envelope of the test building is small.

NBS-114A (REV. 2-8C)

U.S. DEPT. OF COMM. BIBLIOGRAPHIC DATA SHEET (See instructions)	1. PUBLICATION OR REPORT NO. NBS BSS 137	2. Performing Organ. Report No.	3. Publication Date July 1982

4. TITLE AND SUBTITLE

An Evaluation of Thermal Energy Conservation Schemes for an Experimental Masonry Building

5. AUTHOR(S)

Parambir S. Gujral,* Raymond J. Clark,* and Douglas M. Burch

6. PERFORMING ORGANIZATION (If joint or other than NBS, see instructions)

NATIONAL BUREAU OF STANDARDS
DEPARTMENT OF COMMERCE
WASHINGTON, D.C. 20234

*Skidmore, Owings & Merrill
33 W. Monroe Street
Chicago, IL 60603

7. Contract/Grant No.

8. Type of Report & Period Covered

Final

9. SPONSORING ORGANIZATION NAME AND COMPLETE ADDRESS (Street, City, State, ZIP)

Skidmore, Owings & Merrill
33 W. Monroe Street
Chicago, IL 60603

National Bureau of Standards
Washington, DC 20234

King Abdul Aziz University
Makkah Campus
Saudi Arabia

10. SUPPLEMENTARY NOTES

Library of Congress Catalog Card Number: 81-600175

☐ Document describes a computer program; SF-185, FIPS Software Summary, is attached.

11. ABSTRACT (A 200-word or less factual summary of most significant information. If document includes a significant bibliography or literature survey, mention it here)

A one-room masonry building with exterior polystyrene rigid board insulation was built within a large environmental chamber at the National Bureau of Standards. Various climatic conditions were simulated within the chamber, and the transient thermal response of the test building was monitored. Three schemes (night cooling using a ceiling-mounted valance cooling coil, natural ventilation night cooling, and passive solar heating) were investigated with regard to energy conservation. The test results indicated that these operating practices resulted in a considerable reduction in energy consumption for space heating and cooling.

The measured performance of the test building compared favorably with the corresponding performance obtained with an analytic model.

12. KEY WORDS (Six to twelve entries; alphabetical order; capitalize only proper names; and separate key words by semicolons)

building thermal mass; dynamic performance of buildings; energy conservation; heat transfer in buildings; night ventilation; night space cooling; passive solar heating.

13. AVAILABILITY

[X] Unlimited

☐ For Official Distribution. Do Not Release to NTIS

[X] Order From Superintendent of Documents, U.S. Government Printing Office, Washington, D.C. 20402.

☐ Order From National Technical Information Service (NTIS), Springfield, VA. 22161

14. NO. OF PRINTED PAGES

39

15. Price

$4.75

U.S. GOVERNMENT PRINTING OFFICE:1982-375-441

USCOMM-DC 6043-P80

NBS TECHNICAL PUBLICATIONS

PERIODICALS

JOURNAL OF RESEARCH—The Journal of Research of the National Bureau of Standards reports NBS research and development in those disciplines of the physical and engineering sciences in which the Bureau is active. These include physics, chemistry, engineering, mathematics, and computer sciences. Papers cover a broad range of subjects, with major emphasis on measurement methodology and the basic technology underlying standardization. Also included from time to time are survey articles on topics closely related to the Bureau's technical and scientific programs. As a special service to subscribers each issue contains complete citations to all recent Bureau publications in both NBS and non-NBS media. Issued six times a year. Annual subscription: domestic $18; foreign $22.50. Single copy, $4.25 domestic; $5.35 foreign.

NONPERIODICALS

Monographs—Major contributions to the technical literature on various subjects related to the Bureau's scientific and technical activities.

Handbooks—Recommended codes of engineering and industrial practice (including safety codes) developed in cooperation with interested industries, professional organizations, and regulatory bodies.

Special Publications—Include proceedings of conferences sponsored by NBS, NBS annual reports, and other special publications appropriate to this grouping such as wall charts, pocket cards, and bibliographies.

Applied Mathematics Series—Mathematical tables, manuals, and studies of special interest to physicists, engineers, chemists, biologists, mathematicians, computer programmers, and others engaged in scientific and technical work.

National Standard Reference Data Series—Provides quantitative data on the physical and chemical properties of materials, compiled from the world's literature and critically evaluated. Developed under a worldwide program coordinated by NBS under the authority of the National Standard Data Act (Public Law 90-396).

NOTE: The principal publication outlet for the foregoing data is the Journal of Physical and Chemical Reference Data (JPCRD) published quarterly for NBS by the American Chemical Society (ACS) and the American Institute of Physics (AIP). Subscriptions, reprints, and supplements available from ACS, 1155 Sixteenth St., NW, Washington, DC 20056.

Building Science Series—Disseminates technical information developed at the Bureau on building materials, components, systems, and whole structures. The series presents research results, test methods, and performance criteria related to the structural and environmental functions and the durability and safety characteristics of building elements and systems.

Technical Notes—Studies or reports which are complete in themselves but restrictive in their treatment of a subject. Analogous to monographs but not so comprehensive in scope or definitive in treatment of the subject area. Often serve as a vehicle for final reports of work performed at NBS under the sponsorship of other government agencies.

Voluntary Product Standards—Developed under procedures published by the Department of Commerce in Part 10, Title 15, of the Code of Federal Regulations. The standards establish nationally recognized requirements for products, and provide all concerned interests with a basis for common understanding of the characteristics of the products. NBS administers this program as a supplement to the activities of the private sector standardizing organizations.

Consumer Information Series—Practical information, based on NBS research and experience, covering areas of interest to the consumer. Easily understandable language and illustrations provide useful background knowledge for shopping in today's technological marketplace.

Order the **above** *NBS publications from: Superintendent of Documents, Government Printing Office, Washington, DC 20402.*

Order the **following** *NBS publications—FIPS and NBSIR's—from the National Technical Information Services, Springfield, VA 22161.*

Federal Information Processing Standards Publications (FIPS PUB)—Publications in this series collectively constitute the Federal Information Processing Standards Register. The Register serves as the official source of information in the Federal Government regarding standards issued by NBS pursuant to the Federal Property and Administrative Services Act of 1949 as amended, Public Law 89-306 (79 Stat. 1127), and as implemented by Executive Order 11717 (38 FR 12315, dated May 11, 1973) and Part 6 of Title 15 CFR (Code of Federal Regulations).

NBS Interagency Reports (NBSIR)—A special series of interim or final reports on work performed by NBS for outside sponsors (both government and non-government). In general, initial distribution is handled by the sponsor; public distribution is by the National Technical Information Services, Springfield, VA 22161, in paper copy or microfiche form.

U.S. DEPARTMENT OF COMMERCE
National Bureau of Standards
Washington, DC 20234